Involvement of thapsigargin– and cyclopiazonic acid–sensitive pumps in the rescue of TMEM165-associated glycosylation defects by Mn 2+

Marine Houdou, Elodie Lebredonchel, Anne Garat, Sandrine Duvet, Dominique Legrand, Valérie Decool, André Klein, Mohamed Ouzzine, Bruno Gasnier, Sven Potelle, et al.

Involvement of thapsigargin and cyclopiazonic acid sensitive pumps in the rescue of TMEM165-associated glycosylation defects by Mn^{2+}

Marine Houdou[1], Elodie Lebredonchel[1], Anne Garat[2], Sandrine Duvet[1], Dominique Legrand[1], Valérie Decool[2], André Klein[1], Mohamed Ouzzine[3], Bruno Gasnier[4], Sven Potelle*[1] and François Foulquier*[1±]

[1]Univ. Lille, CNRS, UMR 8576 – UGSF - Unité de Glycobiologie Structurale et Fonctionnelle, F-59000 Lille, France

[2] Univ. Lille, CHU Lille, Institut Pasteur de Lille, EA 4483 – IMPECS – IMPact de l'Environnement Chimique sur la Santé humaine, F-59000 Lille, France

[3] UMR 7365 CNRS-Université de Lorraine, Biopôle-Faculté de Médecine, CS 50184, 54505, Vandoeuvre-lès-Nancy, Cedex, France.

[4] Paris Descartes University, Sorbonne Paris Cité, Neurophotonics Laboratory, CNRS UMR8250, 75006 Paris, France.

*These authors shared last authorship

[±]Address correspondence should be sent to: François Foulquier (francois.foulquier@univ-lille1.fr)

Adress : Univ. Lille, CNRS, UMR 8576 – UGSF - Unité de Glycobiologie Structurale et Fonctionnelle, F-59000 Lille, France

Tel. + 33 3 20 43 44 30

Fax. +33 3 20 43 65 55

E-mail. Francois.foulquier@univ-lille1.fr

Short Title: Mechanism of glycosylation rescue in TMEM165 KO cells supplemented with Mn^{2+}

ABBREVIATIONS

Chloroquine: CQ

Congenital Disorders of Glycosylation: CDG

Cyclopiazonic acid: CPA

Inductively Coupled Plasma-Mass Spectrometry: ICP-MS

Lysosomal-associated membrane protein 2: LAMP2

Manganese: Mn

Manganese, ion (2+): Mn^{2+}

Manganese (II) chloride tetrahydrate: $MnCl_2$

Photosynthesis Affected Mutant 71 transporter: PAM71

Sarco/Endoplasmic Reticulum Ca^{2+}-ATPase (SERCA)

Secretory-Pathway Ca^{2+}-ATPase 1: SPCA1

Store Operated Calcium channels: SOC

Superoxide Dismutase: SOD

Thapsigargin: TG

Transmembrane Protein 165: TMEM165

ABSTRACT

Congenital Disorders of Glycosylation (CDG) are severe inherited diseases in which aberrant protein glycosylation is a hallmark.TMEM165 is a novel Golgi transmembrane protein involved in type II CDG. Although its biological function is still a controversial issue, we have demonstrated that the Golgi glycosylation defect due to TMEM165 deficiency resulted from a Golgi Mn^{2+} homeostasis defect. The goal of this study was to delineate the cellular pathway by which extracellular Mn^{2+} rescues N-glycosylation in TMEM165 KO cells.

In this paper, we first demonstrated that after extracellular exposure, Mn^{2+} uptake by HEK293 cells at the plasma membrane did not rely on endocytosis but was likely done by plasma membrane transporters. Second, we showed that the secretory-pathway Ca^{2+}-ATPase 1 (SPCA1), also known to mediate the influx of cytosolic Mn^{2+} into the lumen of the Golgi apparatus, is not crucial for the Mn^{2+} induced rescue glycosylation of LAMP2. In contrast, our results demonstrate the involvement of cyclopiazonic acid (CPA) and thapsigargin (TG) sensitive pumps in the rescue of TMEM165-associated glycosylation defects by Mn^{2+}. Interestingly, overexpression of SERCA2b isoform in TMEM165 KO cells partially rescues the observed LAMP2 glycosylation defect. Overall, this study indicates that the rescue of Golgi N-glycosylation defects in TMEM165 KO cells by extracellular Mn^{2+} involves the activity of TG and CPA sensitive pumps, probably the sarco/endoplasmic reticulum Ca^{2+}-ATPase (SERCA) pumps.

Key words

Manganese homeostasis - Congenital Disorders of Glycosylation – TMEM165 – Golgi apparatus

INTRODUCTION

In 2012, we identified *TMEM165* as a new gene involved in Congenital Disorders of Glycosylation (CDG)(OMIM entry #614727) (1). TMEM165-CDG patients present a peculiar clinical phenotype including major skeletal dysplasia, osteoporosis and dwarfism (2). They also present hyposialylation and hypogalactosylation of their sera N-glycoproteins. TMEM165 is a Golgi transmembrane protein belonging to an uncharacterized family of transmembrane proteins named UPF0016 (Uncharacterized Protein Family 0016; Pfam PF01169). Even if TMEM165 is highly conserved during evolution from yeast to human, its biological function is still a controversial issue. TMEM165 was first described as a Golgi cation antiporter by sequence analogy with other members of the family (3). In addition, we lately demonstrated that the Golgi glycosylation defect due to TMEM165 deficiency in patients and in TMEM165 KO cells resulted from a defect in Golgi Mn^{2+} homeostasis, thus linking TMEM165 with Mn^{2+} homeostasis and suggesting it may import Mn^{2+} into the Golgi stacks (4). This is reinforced by the thylakoid Mn^{2+} import via PAM71, the *Arabidopsis thaliana* ortholog of TMEM165 (5). Besides, we highlighted that only 1µM Mn^{2+} supplementation was sufficient to rescue a normal glycosylation.

Manganese is considered as a trace element but still essential for several cellular processes. It is indeed involved in the catalytic domain of many enzymes such as mitochondrial enzymes, RNA and DNA polymerase and Golgi glycosyltransferases. While the link between Golgi glycosylation and Mn^{2+} is known for long time (6), it was only recently shown that a decrease in cellular Mn^{2+} could cause CDG. In addition with our publication showing that TMEM165 deficiency was linked with Golgi Mn^{2+} homeostasis (4), Park et *al.* have shown that mutations in SLC39A8, a putative plasma membrane manganese transporter, lead to severe glycosylation defects (7).

The question we address here is how does extracellular Mn^{2+} supplementation rescue the glycosylation in TMEM165 KO cells? Extracellular Mn^{2+} could reach the Golgi lumen following two alternative ways: (i) it might be internalized by endocytosis and subsequently reach the Golgi lumen through endosome-to-*trans* Gogi network (TGN) retrograde trafficking (8); (ii) it might cross the plasma membrane and eventually the Golgi membrane through (un)specific channels or transporters. In the latter case, current knowledge suggests that Mn^{2+} supply in the Golgi is achieved via the action of the secretory pathway Ca^{2+}-ATPases (SPCA1 and SPCA2) (9–12), which mediates the import of Ca^{2+} and Mn^{2+} into the Golgi lumen. Thus, the aim of this study was to decipher by which pathways 1µM $MnCl_2$ supplementation leads to glycosylation rescue in TMEM165 KO HEK293 cells.

MATERIAL AND METHODS

Antibodies and other reagents

Anti-TMEM165 and anti-β-Actin antibodies were from Sigma–Aldrich (St Louis, MO, USA). Anti-SPCA1 antibodies were purchased from Abcam (Cambridge, UK) for immunofluorescence staining and from Abnova (Taïwan, China) for Western Blotting. Anti-GM130 antibody was from BD Biosciences (Franklin lakes, NJ, USA). Anti-GPP130 antibody was purchased from Covance (Princeton, NJ, USA) and anti-SERCA2 antibody was purchased from Millipore (Darmstadt, Germany). Polyclonal goat anti-rabbit or goat anti-mouse immunoglobulins HRP conjugated were purchased from Dako (Glostrup, Denmark). Polyclonal goat anti-rabbit or goat anti-mouse conjugated with Alexa Fluor were purchased from Thermo Fisher Scientific (Waltham, MA, USA). Manganese (II) chloride tetrahydrate was from Riedel-de-Haën (Seelze, Germany). All other chemicals were from Sigma-Aldrich unless otherwise specified.

Cell culture, drug treatments and transfections.

Control and TMEM165 KO HEK293 cells were maintained in Dulbecco's Modified Eagle's Medium (DMEM) (Lonza, Basel, Switzerland) supplemented with 10% fetal bovine serum (Dutscher, France), at 37°C in humidity-saturated 5% CO_2 atmosphere. For drug treatments, cells were incubated either with 1µM $MnCl_2$ and/or 10µM chloroquine, 300nM nocodazole, 50nM thapsigargin (TG), 100µM cyclopiazonic acid (CPA), 5mM methyl-β-cyclodextrin (MBCD) for different treatment times as described in each figures and their legends. Transfections were performed using Lipofectamine 2000® (Thermo Scientific) according to the manufacturer's guidelines. Human SERCA2b plasmid (pcDNA3.1+) was purchased from Addgene.

Immunofluorescence staining

Cells were seeded on coverslips for 12 to 24h, treated as indicated in each figures and their legends then washed twice in Phosphate Buffer Saline (PBS, Euromedex) and fixed with 4% paraformaldehyde (PAF) in PBS pH 7.3, for 30 min at room temperature. Coverslips were then washed three times with PBS and cells were permeabilized with 0.5% Triton X-100 in PBS for 10 min before being washed three times with PBS. Coverslips were then incubated for 1h in blocking buffer [0.2% gelatin, 2% Bovin Serum Albumin (BSA), 2% Fetal Bovine Serum (FBS) (Lonza) in PBS] and then for 1h with primary antibody diluted either at 1:100 or 1:300 in blocking buffer. After three washing with PBS, cells were incubated for 1h with Alexa 488- or Alexa 568-conjugated secondary antibody (Life Technologies) diluted at 1:600 in blocking buffer. After three

washing with PBS, coverslips were mounted on glass slides with Mowiol. Fluorescence was detected through an inverted Zeiss LSM780 or LSM700 confocal microscope. Acquisitions were done using the ZEN pro 2.1 software (Zeiss, Oberkochen, Germany).

Image Analyses

Immunofluorescence images were analyzed using TisGolgi, a homemade imageJ (http://imagej.nih.gov/ij) plugin developed by the local TISBio facility (http://tisbio.wixsite.com/tisbio) and available upon request. Basically, the program automatically detects and discriminates Golgi and vesicles, based on morphological parameters such as size and sphericity. Then, the program calculates for each image the number of detected objects, their size and mean fluorescence intensity.

Western Blotting

Cells were scraped in DPBS and then centrifuged at 4000g , 4°C for 10 min. Supernatant was discarded and cells were then resuspended in RIPA buffer [Tris/HCl 50mM pH 7.9, NaCl 120mM, NP40 0.5%, EDTA 1mM, Na_3VO_4 1mM, NaF 5mM] supplemented with a protease cocktail inhibitor (Roche Diagnostics, Penzberg, Germany). Cell lysis was done either by passing the cells several times through a syringe with a 26G needle or by a sonication bath for 2 min followed by incubation on ice for 10 min. Cells were centrifuged for 30 min, 4°C at 20 000g. Protein concentration contained in the supernatant was estimated with the micro BCA Protein Assay Kit (Thermo Scientific). 10 or 20µg of total protein lysate were mixed with NuPAGE LDS sample buffer (Invitrogen) pH 8.4 supplemented with 4% β-mercaptoethanol (Fluka). Samples were heated 10 min at 95°C (excepted for TMEM165, SPCA1 and SERCA2) then separated on 4%-12% Bis-Tris gels (Invitrogen) and transferred to nitrocellulose membrane Hybond ECL (GE Healthcare, Little Chalfont, UK). Membranes were blocked in blocking buffer (5% milk powder in TBS-T [1X TBS with 0.05% Tween20]) for 1h at room temperature, then incubated overnight with the primary antibodies (used at a dilution of 1:1000) in blocking buffer and washed three times for 5 min in TBS-T. Membranes were then incubated with the peroxidase-conjugated secondary goat anti-rabbit or goat anti-mouse antibodies (Dako; used at a dilution of 1:10,000 or 1:20,000) in blocking buffer for 1h at room temperature and later washed three times for 5 min in TBS-T. Signal was detected with chemiluminescence reagent (ECL 2 Western Blotting Substrate or SuperSignal West Pico PLUS chemiluminescent Substrate, Thermo Scientific) on imaging film (GE Healthcare, Little Chalfont, UK).

Mass spectrometry

2 T75 flasks at 90% confluence, treated as indicated in each figures and their legends were used. Cells were then scraped in DPBS at 4°C and centrifuged at 4000g, 4°C for 5min. Then, supernatant was discarded, cells were resuspended in PBS and washed 4 times by centrifugation (4000g, 4°C for 10min). Before the last wash, an aliquot of the resuspended cells in PBS has been kept (1:10) in order to estimate the total protein concentration of the sample. The resting pellets were resuspended in lysis buffer (1% Triton-X100 in PBS) following a sonication bath at 4°C for 1h and centrifuged at 20 000g, 4°C for 10min. Supernatants were then transferred into new tubes. Next, dithiotreitol (Sigma-Aldrich, MO, USA) was added to a final concentration of 10mM and incubated 45min at 56°C followed by the addition of 50mM iodoacetamide (Bio-Rad) for 1h at 37°C, protected from the light. The reduced and acylated proteins were precipitated with a final concentration of 10% trichloroacetic acid and incubated for 30min at -20°C. After a centrifugation at 20 000g, 4°C for 10min, supernatants were discarded. Protein pellets were then washed by the addition of iced-acetone and centrifuged at 20 000g, 4°C for 10min. This step was repeated. Washed proteins pellets were dried at room temperature for 30min. Then, trypsin at 2mg/mL (Sigma-Aldrich, MO, USA) was added overnight and up to 48h at 37°C in 50mM ammonium bicarbonate (Sigma-Aldrich, MO, USA) with a 5:1 ratio. The reaction was stopped by heating samples 10min at 100°C. N-glycans were released from the proteins by addition of 10 units of PNGase F (Roche) overnight, at 37°C. N-glycans were then purified by a C18 Sep-Pak chromatography (Water Corp., Guyancourt, France). The column was washed with 100% acetonitrile and 100% 2-propanol, and then equilibrated with 5% acetic acid in water. Samples were loaded onto the C18 Sep-Pak and the bound peptides were eluted three times with 5% acetic acid in water. N-glycans in 5% aqueous acetic acid were lyophylized overnight. They were permethylated and spotted onto MALDI plate and analyzed using MALDITOF/TOF analyzed on 4800 Proteomics Analyzer mass spectrometer (Applied Biosystems, Framingham, MA, USA), as described in Delannoy et *al.*, 2016 (13). Each spectrum resulted from the accumulation of 10 000 spectra and shows glycans structures from mass-per-charge ratio (m/z) 1500 up to 3000.

Whole cell Mn measurement by ICP-MS

Sample preparation

After the indicated treatments, cells were washed twice in DPBS at 4°C. Cells were then harvested and centrifuged at 4000g, 4°C for 10 min. Supernatant was discarded and cells were then

resuspended in 1mL of PBS: 200µL were kept for protein dosage and 800µL were kept for manganese (Mn) measurement by ICP-MS (Inductively Coupled Plasma - Mass Spectrometer). Both were centrifuged at 4000g, 4°C for 10 min. Cell pellet for protein dosage was resuspended in RIPA buffer and cell lysis was performed as indicated in the Western Blotting section. Protein concentration contained in the supernatant was estimated with the micro BCA Protein Assay Kit (Thermo Scientific). Cell pellet for ICP-MS analysis was resuspended in deionized water and then sonicated for 30 seconds. A chloroform/methanol/water (ratio 2:1:3) extraction was then done to separate lipids, proteins and soluble material. The upper phase containing soluble material was kept and dried out under nitrogen flux or with a vacuum concentrator (Eppendorf concentrator 5301). Samples were then dissolved in 500µL of deionized water.

Instrumentation and analysis

Samples were diluted 50 times with 1,5% (v/v) nitric acid (ultrapure quality 69,5%, Carlo Erba Reagents, Val de Reuil, France) solution in ultrapure water (Purelab Option-Q, Veolia Water, Antony, France) containing 0,1% TritonX-100 (Euromedex, Souffelweyersheim, France), 0,2% butan-1-ol (VWR Chemicals, Fontenay-sous-Bois, France), and 0,5µg/L rhodium (Merk, Darmstadt, Germany). Assays were performed on an ICP-MS THERMO ICAP^{TM} Q (Thermo Scientific, Courtaboeuf Cedex, France).The limit of quantification was 0,2µg/L.

Statistical Analysis

Comparisons between groups were performed using Student t-test for 2 variables with equal or different variances, depending on the result of the F-test.

RESULTS

Time course of the rescue of LAMP2 glycosylation by Mn^{2+}

Our previous studies demonstrated that supplementation with low Mn^{2+} concentrations could completely suppress LAMP2 glycosylation defects in TMEM165 KO cells (4). This has however been observed for long treatments (48h). The time course of the Mn^{2+} effect was not evaluated. To answer this point, a concentration of 1µM of $MnCl_2$ was applied to the cells for increasing times (1h to 64h) and LAMP2 glycosylation was assessed by western blotting (Fig. 1A). The results show that following Mn^{2+} treatment of TMEM165 KO cells, fully glycosylated forms of LAMP2 appear after 8h of Mn^{2+} treatment, yet most LAMP2 remain underglycosylated. Relative quantification of underglycosylated and fully glycosylated LAMP2 (Fig. 1B) indicates that fully glycosylated LAMP2 progressively increases from 10% of LAMP2 after 8h to 97% after 64h of Mn^{2+} treatment. This result is consistent with the slow turnover of LAMP2 estimated to 48h. In further experiments, cells were treated with 1µM $MnCl_2$ for 8 and/or 16h.

Blocking endocytosis in TMEM165 KO cells does not prevent the rescue of LAMP2 glycosylation by Mn^{2+}

The pathways by which Mn^{2+} enters cells after $MnCl_2$ exposure are unknown. Two different ways are possible, either by permeating membranes using specific and/or unspecific transporters or via endocytosis and endosome-to-TGN retrograde trafficking (8). To discriminate between these possibilities, cells were treated with different drugs known to interfere with endocytosis such as chloroquine (CQ) (14), a weak base raising the pH of acidic compartments, methyl-β-cyclodextrin (MBCD) that depletes cholesterol from plasma membrane and nocodazole, a microtubule depolymerizing agent (15) (Fig.2 and supplementary Fig. 1 and 2). We first checked the potential effects of these drugs on both the steady-state glycosylation status of LAMP2 in control HEK293 cells and the subcellular localization of LAMP2. No changes in the LAMP2 electrophoresis mobility could be observed in control HEK293 cells after these drug treatments (supplementary Fig. 1A and 2A), suggesting no major alteration of its glycosylation. Moreover, neither nocodazole or methyl-β-cyclodextrin nor chloroquine disrupted the lysosomal localization of LAMP2 (supplementary Fig. 1B and 2B).

We also checked the effects of those drugs on the morphology of the Golgi apparatus. Immunofluorescence staining of the Golgi proteins GPP130 and GM130 were performed followed by confocal microscopy analyses (supplementary Fig. 1B and 2B). As already known from the literature, nocodazole fragmented the Golgi apparatus whereas CQ and MBCD had no effect on its morphology.

LAMP2 glycosylation profile in TMEM165 KO HEK293 cells after treatment with or without a combination of those drugs and $MnCl_2$ was then assessed (Fig. 2 and supplementary Fig. 2C). The observed LAMP2 mobility in TMEM165 KO cells after 1µM $MnCl_2$ treatment was comparable to the one observed in Fig. 1. 10% of LAMP2 was found to be normally glycosylated after 8h of Mn^{2+} treatment and 33% after 16h. Cells were then treated with CQ or MBCD in the presence or absence of 1µM $MnCl_2$ for 8h and 16h (Fig. 2). The result shows that CQ and MBCD did not prevent the rescue of LAMP2 glycosylation after Mn^{2+} supplementation as 22% and 32% of fully glycosylated forms respectively are observed after 16h treatment. Similar results were obtained with nocodazole (supplementary Fig.1C, D).

In conclusion, these results clearly highlight that none of these drugs prevents the rescue of LAMP2 glycosylation by Mn^{2+} in TMEM165 KO cells. This suggests that, at the extracellular concentration used in our study (1µM), Mn^{2+} enter TMEM165-defective HEK293 cells through plasma membrane transporters rather than by endocytosis.

Is the Golgi pump SPCA1 involved in the Mn^{2+}-induced rescue of LAMP2 glycosylation?

After entering TMEM165-defective cells, cytosolic Mn^{2+} should reach the Golgi lumen to correct the glycosylation defects. Besides TMEM165, which acts as a key determinant for Golgi Mn^{2+} homeostasis (4), the SPCA pumps (SPCA1 and SPCA2) are known to be the main suppliers of Mn^{2+} in the Golgi lumen (11). As SPCA2 is poorly expressed in our cell line, we tested the contribution of SPCA1 by silencing its gene, *ATP2C1* (Fig. 3). SiRNA knockdown was very efficient as 95% of the protein was depleted compared to untreated cells. Surprisingly, the knockdown of *ATP2C1* did not prevent the rescue of LAMP2 glycosylation by Mn^{2+}. 37% of LAMP2 was fully glycosylated after 16h Mn^{2+} treatment in si*ATP2C1*-treated cells, a level similar to that observed without *ATP2C1* knockdown. SPCA1 is thus not involved in the glycosylation rescue induced by Mn^{2+} supplementation in TMEM165 KO HEK293 cells.

Golgi glycosylation rescue induced by Mn^{2+}supplementation requires TG and CPA sensitive

pumps

Given the previous results, we next considered whether the ER could play a role in the observed glycosylation rescue. It had indeed been shown that SERCA pumps are able, in certain conditions, to transport Mn^{2+} into the ER lumen in addition to Ca^{2+} (16–18). We thus hypothesized that SERCA pumps might be involved in the Mn^{2+} supplementation effect. To address this point, LAMP2 glycosylation status was evaluated by western blotting in cells treated with cyclopiazonic acid (CPA) or thapsigargin (TG), two specific SERCA inhibitors, in presence or absence of 1µM $MnCl_2$ (Fig. 4). We can first notice that CPA as well as TG, did not induce any glycosylation defect on LAMP2 in control HEK293 cells neither after 8 nor 16h of treatment (supplementary Fig. 3). Remarkably, in TMEM165 KO HEK293 cells treated with CPA and 1µM $MnCl_2$, the treatment strongly delays the rescue of LAMP2 glycosylation by Mn^{2+} as only 4% of LAMP2 was fully glycosylated after 8h and 29% after 16h of Mn^{2+} treatment. To reinforce this result, stronger effects were obtained after TG treatment (Fig. 4A, B). To confirm these results at the structural level, mass spectrometry of total N-glycans have been performed (Fig. 5). For this, TMEM165 KO HEK293 cells were treated or not with 1µM $MnCl_2$ and with or without TG/CPA. Consistent with our previous studies, a pronounced hypogalactosylation was seen in TMEM165 KO HEK293 cells, with the accumulation of agalactosylated glycan structures detected at mass-per-charge (m/z) ratios 1661, 1835, 2081 and 2326. Consistent with our previous studies, $MnCl_2$ treatment rescues the general glycosylation defect as indicated by the decreased abundance of the structures (m/z) 1835, 2081 and 2326 (54% decrease, supplementary Fig. 4). Although TG and CPA treatments in KO TMEM165 cells slightly increase the abnormal agalactosylated glycan structures, such treatments fully prevent the total rescue of TMEM165-associated glycosylation defects by Mn^{2+} as indicated by the remaining high abundance of the structures (m/z) 1661, 1835, 2081 and 2326 (supplementary Fig. 4).

To validate these results, we tested whether CPA or TG treatment acted by indirectly altering Mn^{2+} entry into the cells. Therefore, the total cellular Mn concentration in presence and absence of CPA or TG was evaluated by Inductively Coupled Plasma-Mass Spectrometry (ICP-MS) after $MnCl_2$ supplementation. The result shows that after Mn^{2+} supplementation, the amount of Mn is comparable in cells treated or not with CPA or TG (supplementary Fig. 3C). This demonstrates that neither CPA nor TG prevented the cellular Mn^{2+} entry after $MnCl_2$ supplementation.

In parallel, the effects of CPA and TG on the morphology of the Golgi apparatus were investigated confocal immunofluorescence analysis of the Golgi proteins GPP130 and GM130 (Fig. 4C and supplementary Fig. 3A). No effect was observed on the Golgi apparatus morphology after CPA

treatment and only a slight dilatation of the Golgi was shown after TG treatment. Moreover, LAMP2 localization was not disrupted neither by TG nor CPA.

Overall, these results provide pharmacological evidences for the involvement of TG and CPA sensitive pumps in the Golgi N-glycosylation rescue induced by Mn^{2+} supplementation in TMEM165 KO HEK293 cells.

Potential involvement of SERCA pump in the Mn^{2+} -induced rescue of LAMP2 glycosylation

The observed TG and CPA sensitivity led us to investigate the potential role of ER SERCA pump in the Mn^{2+} supplementation effect. Amongst all SERCA proteins, the SERCA2b isoform is the main form expressed in HEK cells. SERCA2b was overexpressed for 48h in TMEM165 KO HEK293 cells and LAMP2 glycosylation status was assayed by western blot. The correct SERCA2b expression has been checked by immunofluorescence (data not shown) and western blot analyses in both TMEM165 KO and control HEK293 cells (Fig. 6). Compared to untransfected cells, LAMP2 glycosylation profile is slightly restored in TMEM165 KO HEK293 cells overexpressing SERCA2b (Fig. 6). In order to prove that this slight rescue was not due to potential ER/Golgi Ca^{2+} homeostasis changes, the overexpressing cells were treated with 500µM $CaCl_2$ and 1mM sodium pyruvate. LAMP2 glycosylation rescue is identical to the one obtained without such treatment and suggests that the observed shift is likely not the cause of the SERCA2b Ca^{2+} pumping activity. Altogether these results suggest the potential involvement of SERCA2b pump in the Mn^{2+} rescued glycosylation of LAMP2.

DISCUSSION

TMEM165 deficiency was recently found to lead to a type-II CDG associated with strong Golgi glycosylation abnormalities (1). Our previous work has shown that these glycosylation abnormalities in TMEM165 KO cells could result from a lack of Golgi Mn^{2+} (4). Many Golgi glycosyltransferases using UDP-sugars as a donor substrate, such as UDP-Gal:N-acetylglucosamine β-1,4-galactosyltransferase I (B4GALT1; EC 2.4.1.22) and UDP-Gal:N-acetylglucosamine β-1,4-galactosyltransferase II (B4GALT2; EC 2.4.1.22), are indeed known to require Mn^{2+} in their catalytic site to be fully active. Indeed, as well described by Ramakrishnan et *al*. (19), Mn^{2+} first needs to bind the enzyme in a so-called open conformation to then allow the binding of the nucleotide sugar. Once in this enzyme-Mn^{2+}-nucleotide sugar conformation, the acceptor substrates bind it and the catalysis can start. Remarkably, we have demonstrated that 1µM $MnCl_2$ supplementation was sufficient to completely suppress the glycosylation defects in TMEM165 KO cells. The underlying mechanism of this glycosylation rescue by $Mn^{2+}$was however unknown.
To address this point, LAMP2 was used as a reporter glycoprotein to finely study the Mn^{2+} induced mechanism of Golgi glycosylation rescue. We have clearly shown that after 8h 1µM $MnCl_2$ treatment, newly synthesized LAMP2 was already fully glycosylated in TMEM165 KO cells. Moreover and in line with its turnover, half of LAMP2 is fully glycosylated after 24h treatment and almost all LAMP2 is fully glycosylated after 64h treatment. This showed that LAMP2 could be used to study glycosylation kinetics and that 1µM $MnCl_2$ was able to totally suppress the glycosylation defect observed on LAMP2 in TMEM165 KO HEK293 cells.

The first step of this glycosylation rescue induced by 1µM $MnCl_2$ is the Mn^{2+} uptake at the plasma membrane. This can be done either by endocytosis or through transporters. Using CQ, nocodazole and MBCD, three drugs known to disrupt endocytosis (14), we have demonstrated that none of these drugs prevented the glycosylation rescue after 1µM $MnCl_2$ exposure in TMEM165 KO cells, then suggesting that Mn^{2+} does not enter into cells via endocytosis. This can easily be explained by the presence of several plasma membrane transporters known to import Mn^{2+}. This includes the divalent metal transporter 1 (DMT1/NRAMP2/SLC11A2) (20, 21), NRAMP1 (22), the transferrin, the transporters SLC30A10/ZNT8 (23), SLC39A8/ZIP8 (7) and SLC30A14/ZIP14 (24, 25). As a consequence, we can reasonably think that Mn^{2+}can use a wide set of transporters to directly enter into cells, thus making the identification of the involved transporters difficult with possibly different answers depending on the cell type.

Once in the cytosol, Mn^{2+} needs to reach the Golgi lumen to suppress the Golgi glycosylation defect induced by a lack of TMEM165. In absence of TMEM165, it is likely that Mn^{2+} supply in the Golgi is achieved via the action of SPCA pumps (SPCA1 and SPCA2) (9, 11, 26). Overexpression of SPCA1 has indeed been shown to increase Mn^{2+} accumulation into the Golgi after high Mn^{2+} concentrations exposure (27). Given SPCA2 is not expressed in HEK cells, we have depleted SPCA1 by siRNA and analysed the status of LAMP2 glycosylation in TMEM165 KO cells in the presence or absence of 1µM $MnCl_2$. The results unequivocally showed that Mn^{2+} supplementation could rescue a normal LAMP2 glycosylation in si*ATP2C1* TMEM165 KO treated cells. This demonstrates that somehow, SPCA1 is not involved in the glycosylation rescue induced by Mn^{2+} in TMEM165 KO cells. However, since 5% of SPCA1 still remains after siRNA treatment, we cannot completely exclude that the remaining SPCA1 is sufficient to efficiently transport Mn^{2+} from the cytosol to the Golgi apparatus to rescue glycosylation.

We then investigated the hypothesis that Mn^{2+} could reach the ER before being transported to the Golgi compartment. The effects of specific inhibitors of sarcoplasmic reticulum (SR) calcium ATPase, thapsigargin (TG), and cyclopiazonic acid (CPA) were investigated. Interestingly, we did demonstrate that Mn^{2+} supplementation could not rescue a correct LAMP2 glycosylation in cells treated with CPA (100µM) or TG (50nM). Importantly, these used concentrations of CPA and TG did not inhibit the activity of SPCA1. Indeed, Chen *et al*., recently showed that SPCA1 inhibition by either CPA or TG occurred from 182µM and 7µM, respectively (28). As we demonstrated using ICP-MS that neither CPA nor TG treatment prevented the cellular Mn^{2+} entry, our results suggests that the observed Golgi glycosylation rescue induced by Mn^{2+} supplementation could come from ER/Golgi uptake via TG and CPA sensitive proteins. To address the potential involvement of SERCA pumps, SERCA2b (the main isoform expressed in HEK cells) overexpression in TMEM165 KO HEK293 cells was performed. Although partial, the LAMP2 glycosylation profile is clearly enhanced then suggesting the involvement of SERCA2b protein in the Mn^{2+} rescued glycosylation of LAMP2.

The importance of SERCA pumps in the observed Golgi glycosylation rescue was quite unexpected and the molecular mechanisms by which SERCA pumps are involved in the Mn^{2+} rescued Golgi glycosylation in TMEM165 KO cells remain unknown. One can expect that under Mn^{2+} supplementation, cytosolic Mn^{2+} is directly pumped by SERCA into the ER. Such role has already been documented in literature. Chiesi *et al* showed in sarcoplasmic reticulum vesicles that a Ca^{2+} ATPase could indeed be activated by Mn^{2+} and was even able to import Mn^{2+} instead of Ca^{2+}, but at slower rate (17). It has also been confirmed many years ago that SERCA1a was able to

transport Mn^{2+} instead of Ca^{2+} with similar activation energies, same mechanism but with a much lower affinity (18). Another hypothesis that we can't exclude would be the crucial importance of ER/Golgi Ca^{2+} homeostasis in the Mn^{2+} induced Golgi glycosylation rescue. Some Golgi glycosyltransferases and particularly the Golgi β4GalT1 (EC 2.4.1.38) enzyme possesses two metal binding sites, the site I that binds Mn^{2+} with high affinity and site II that binds diverse metal ions including Ca^{2+} (18). It could be possible that a decrease in ER/ Golgi Ca^{2+} homeostasis completely inhibits, *in cellulo*, the activity of β4GalT1 even under Mn^{2+} supplementation.

Overall, this paper shed light on the involvement of thapsigargin and cyclopiazonic acid sensitive pumps, most likely SERCA pump, in the rescue of TMEM165-associated glycosylation defects by Mn^{2+}.

Acknowledgments

We are indebted to Dounia Mouajjah for her helpful assistance in mass spectrometry experiments. We also acknowledge Dr Dominique Legrand for the Research Federation FRABio (Univ. Lille, CNRS, FR 3688, FRABio, Biochimie Structurale et Fonctionnelle des Assemblages Biomoléculaires) for providing the scientific and technical environment conducive to achieving this work. We thank the BioImaging Center of Lille, especially Christian Slomianny and Elodie Richard, for the use of the Leica LSM700 and the Leica LSM780.

Conflict of interests

None.

Funding

'This work was supported by the French National Research Agency [SOLV-CDG to F.F]; and the Mizutani Foundation for Glycoscience [to F.F].

Author contributions

F. Foulquier and S. Potelle designed the research; M. Houdou, E. Lebredonchel, V. Decool. M. Houdou, S. Potelle and S. Duvet analyzed data; M. Houdou, S. Potelle and F. Foulquier wrote the paper. A. Garat and D. Allorge developed and optimized the ICP-MS analysis and kindly gave us access to the platform for our experiments. D. Legrand, A. Klein, B. Gasnier and M. Ouzzine helped editing the paper and provided useful advices.

References

1. Foulquier, F., Amyere, M., Jaeken, J., Zeevaert, R., Schollen, E., Race, V., Bammens, R., Morelle, W., Rosnoblet, C., Legrand, D., Demaegd, D., Buist, N., Cheillan, D., Guffon, N., Morsomme, P., Annaert, W., Freeze, H. H., Van Schaftingen, E., Vikkula, M., and Matthijs, G. (2012) TMEM165 Deficiency Causes a Congenital Disorder of Glycosylation. *Am. J. Hum. Genet.* **91**, 15–26

2. Zeevaert, R., de Zegher, F., Sturiale, L., Garozzo, D., Smet, M., Moens, M., Matthijs, G., and Jaeken, J. (2013) Bone Dysplasia as a Key Feature in Three Patients with a Novel Congenital Disorder of Glycosylation (CDG) Type II Due to a Deep Intronic Splice Mutation in TMEM165. *JIMD Rep.* **8**, 145–152

3. Demaegd, D., Foulquier, F., Colinet, A.-S., Gremillon, L., Legrand, D., Mariot, P., Peiter, E., Van Schaftingen, E., Matthijs, G., and Morsomme, P. (2013) Newly characterized Golgi-localized family of proteins is involved in calcium and pH homeostasis in yeast and human cells. *Proc. Natl. Acad. Sci.* **110**, 6859–6864

4. Potelle, S., Morelle, W., Dulary, E., Duvet, S., Vicogne, D., Spriet, C., Krzewinski-Recchi, M.-A., Morsomme, P., Jaeken, J., Matthijs, G., De Bettignies, G., and Foulquier, F. (2016) Glycosylation abnormalities in Gdt1p/TMEM165 deficient cells result from a defect in Golgi manganese homeostasis. *Hum. Mol. Genet.* **25**, 1489–1500

5. Schneider, A., Steinberger, I., Herdean, A., Gandini, C., Eisenhut, M., Kurz, S., Morper, A., Hoecker, N., Rühle, T., Labs, M., Flügge, U.-I., Geimer, S., Schmidt, S. B., Husted, S., Weber, A. P. M., Spetea, C., and Leister, D. (2016) The Evolutionarily Conserved Protein PHOTOSYNTHESIS AFFECTED MUTANT71 Is Required for Efficient Manganese Uptake at the Thylakoid Membrane in Arabidopsis. *Plant Cell* **28**, 892–910

6. Powell, J. T. and Brew, K. (1976) Metal ion activation of galactosyltransferase. *J. Biol. Chem.* **251**, 3645–3652

7. Park, J. H., Hogrebe, M., Grüneberg, M., DuChesne, I., von der Heiden, A. L., Reunert, J., Schlingmann, K. P., Boycott, K. M., Beaulieu, C. L., Mhanni, A. A., Innes, A. M., Hörtnagel, K., Biskup, S., Gleixner, E. M., Kurlemann, G., Fiedler, B., Omran, H., Rutsch, F., Wada, Y., Tsiakas, K., Santer, R., Nebert, D. W., Rust, S., and Marquardt, T. (2015) SLC39A8 Deficiency: A Disorder of Manganese Transport and Glycosylation. *Am. J. Hum. Genet.* **97**, 894–903

8. Bonifacino, J. S. and Rojas, R. (2006) Retrograde transport from endosomes to the trans-Golgi network. *Nat. Rev. Mol. Cell Biol.* **7**, 568–579

9. He, W. and Hu, Z. (2012) The role of the Golgi-resident SPCA Ca^{2+}/Mn^{2+} pump in ionic homeostasis and neural function. *Neurochem. Res.* **37**, 455–468

10. Micaroni, M., Perinetti, G., Berrie, C. P., and Mironov, A. A. (2010) The SPCA1 Ca2+ pump and intracellular membrane trafficking. *Traffic Cph. Den.* **11**, 1315–1333

11. Van Baelen, K., Dode, L., Vanoevelen, J., Callewaert, G., De Smedt, H., Missiaen, L., Parys, J. B., Raeymaekers, L., and Wuytack, F. (2004) The Ca2+/Mn2+ pumps in the Golgi apparatus. *Biochim. Biophys. Acta* **1742**, 103–112

12. Roth, J. A. (2006) Homeostatic and toxic mechanisms regulating manganese uptake, retention, and elimination. *Biol. Res.* **39**, 45–57

13. Delannoy, C. P., Rombouts, Y., Groux-Degroote, S., Holst, S., Coddeville, B., Harduin-Lepers, A., Wuhrer, M., Elass-Rochard, E., and Guérardel, Y. (2017) Glycosylation Changes Triggered by the Differentiation of Monocytic THP-1 Cell Line into Macrophages. *J. Proteome Res.* **16**, 156–169

14. Dutta, D. and Donaldson, J. G. (2012) Search for inhibitors of endocytosis. *Cell. Logist.* **2**, 203–208

15. Bayer, N., Schober, D., Prchla, E., Murphy, R. F., Blaas, D., and Fuchs, R. (1998) Effect of Bafilomycin A1 and Nocodazole on Endocytic Transport in HeLa Cells: Implications for Viral Uncoating and Infection. *J. Virol.* **72**, 9645–9655

16. Chiesi, M. and Inesi, G. (1980) Adenosine 5'-triphosphate dependent fluxes of manganese and and hydrogen ions in sarcoplasmic reticulum vesicles. *Biochemistry (Mosc.)* **19**, 2912–2918

17. Chiesi, M. and Inesi, G. (1981) Mg2+ and Mn2+ modulation of Ca2+ transport and ATPase activity in sarcoplasmic reticulum vesicles. *Arch. Biochem. Biophys.* **208**, 586–592

18. Yonekura, S.-I. and Toyoshima, C. (2016) Mn2+ transport by Ca2+-ATPase of sarcoplasmic reticulum. *FEBS Lett.* **590**, 2086–2095

19. Ramakrishnan, B., Ramasamy, V., and Qasba, P. K. (2006) Structural snapshots of beta-1,4-galactosyltransferase-I along the kinetic pathway. *J. Mol. Biol.* **357**, 1619–1633

20. Au, C., Benedetto, A., and Aschner, M. (2008) Manganese transport in eukaryotes: the role of DMT1. *Neurotoxicology* **29**, 569–576

21. Garrick, M. D., Dolan, K. G., Horbinski, C., Ghio, A. J., Higgins, D., Porubcin, M., Moore, E. G., Hainsworth, L. N., Umbreit, J. N., Conrad, M. E., Feng, L., Lis, A., Roth, J. A., Singleton, S., and Garrick, L. M. (2003) DMT1: a mammalian transporter for multiple metals. *Biometals Int. J. Role Met. Ions Biol. Biochem. Med.* **16**, 41–54

22. Forbes, J. R. and Gros, P. (2003) Iron, manganese, and cobalt transport by Nramp1 (Slc11a1) and Nramp2 (Slc11a2) expressed at the plasma membrane. *Blood* **102**, 1884–1892

23. Chen, P., Bowman, A. B., Mukhopadhyay, S., and Aschner, M. (2015) SLC30A10: A novel manganese transporter. *Worm* **4**, e1042648

24. Chen, P., Chakraborty, S., Mukhopadhyay, S., Lee, E., Paoliello, M. M. B., Bowman, A. B., and Aschner, M. (2015) Manganese homeostasis in the nervous system. *J. Neurochem.* **134**, 601–610

25. Girijashanker, K., He, L., Soleimani, M., Reed, J. M., Li, H., Liu, Z., Wang, B., Dalton, T. P., and Nebert, D. W. (2008) Slc39a14 gene encodes ZIP14, a metal/bicarbonate symporter: similarities to the ZIP8 transporter. *Mol. Pharmacol.* **73**, 1413–1423

26. Vandecaetsbeek, I., Vangheluwe, P., Raeymaekers, L., Wuytack, F., and Vanoevelen, J. (2011) The Ca2+ Pumps of the Endoplasmic Reticulum and Golgi Apparatus. *Cold Spring Harb. Perspect. Biol.* **3**, a004184–a004184

27. Mukhopadhyay, S. and Linstedt, A. D. (2011) Identification of a gain-of-function mutation in a Golgi P-type ATPase that enhances Mn2+ efflux and protects against toxicity. *Proc. Natl. Acad. Sci. U. S. A.* **108**, 858–863

28. Chen, J., De Raeymaecker, J., Hovgaard, J. B., Smaardijk, S., Vandecaetsbeek, I., Wuytack, F., Møller, J. V., Eggermont, J., De Maeyer, M., Christensen, S. B., and Vangheluwe, P. (2017) Structure/activity relationship of thapsigargin inhibition on the purified Golgi/secretory pathway Ca^{2+} /Mn^{2+} -transport ATPase (SPCA1a). *J. Biol. Chem.* **292**, 6938–6951

Legends to figures

Figure 1: Time course of the Mn^{2+} induced LAMP2 glycosylation rescue. A. Control and TMEM165 KO HEK293 cells were cultured with 1µM $MnCl_2$ during the indicated times. Cell culture medium was renewed every 16h. Total cell lysates were prepared, subjected to SDS-PAGE and western blot with the indicated antibodies. **B.** Relative quantification of fully and underglycosylated forms of LAMP2 (N, number of experiments = 2).

Supplementary figure 1: Effect of chloroquine (CQ) on Golgi morphology, LAMP2 subcellular localization and glycosylation profile. A. Control HEK293 cells were incubated with CQ (10µM) for 8h or 16h, in combination or not with 1µM $MnCl_2$. Total cell lysates were prepared, subjected to SDS-PAGE and western blot with the indicated antibodies. **B**. Immunofluorescence analysis. Control and TMEM165 KO HEK293 cells were incubated with CQ (10µM) for 16h, fixed, permeabilized and labeled with antibodies against GM130, GPP130 and LAMP2 before confocal microscopy visualization. DAPI staining (blue) was performed, showing nuclei.

Supplementary figure 2: Effect of nocodazole on Golgi morphology, LAMP2 subcellular localization and glycosylation profile. A. and **C.** Control and TMEM165 KO HEK293 cells were incubated with nocodazole (300nM) for 8h or 16h, in combination or not with 1µM $MnCl_2$. Total cell lysates were prepared, subjected to SDS-PAGE and western blot with the indicated antibodies. **B**. Immunofluorescence analysis. Control and TMEM165 KO HEK293 cells were incubated with nocodazole (300nM) for 16h, fixed, permeabilized and labeled with antibodies against GM130, GPP130 and LAMP2 before confocal microscopy visualization. DAPI staining (blue) was performed, showing nuclei. **D.** Relative quantification of fully and underglycosylated forms of LAMP2 (N, number of experiments = 2).

Figure 2: Mn^{2+} entry into TMEM165 KO HEK293 cells does not rely on endocytosis. A. Control and TMEM165 KO HEK293 cells were cultured with CQ (10µM) in combination or not with 1µM $MnCl_2$ for 8h or 16h. Total cell lysates were prepared, subjected to SDS-PAGE and western blot with the indicated antibodies. **B.** Relative quantification of fully and underglycosylated forms of LAMP2 (N, number of experiments = 2).

Figure 3: *ATP2C1* knockdown does not prevent the Mn^{2+} induced rescue glycosylation of LAMP2 in TMEM165 KO HEK293 cells. A. Control, TMEM165 KO and si*ATP2C1* HEK293 cells were cultured with 1µM $MnCl_2$ for 16h. Total cell lysates were prepared, subjected to SDS-PAGE and western blot with the indicated antibodies. **B.** Quantification of SPCA1 protein expression after normalization with actin. **C**. Relative quantification of fully and underglycosylated forms of LAMP2.

Figure 4: Involvement of TG and CPA sensitive pumps in the Mn^{2+} induced rescue of LAMP2 glycosylation. A. Control cells were cultured with either thapsigargine (TG) (50nM) or cyclopiazonic acid (CPA) (100µM), two SERCA inhibitors, in combination or not with 1µM $MnCl_2$ for 8h or 16h. Total cell lysates were prepared, subjected to SDS-PAGE and western blot with the indicated antibodies. **B.** Relative quantification of fully and underglycosylated forms of LAMP2 (N,

number of experiment = 2). **C.** Immunofluorescence analysis. TMEM165 KO HEK293 cells were incubated with either TG (50nM) or CPA (100µM) for 16h, fixed, permeabilized and labeled with antibodies against GM130, GPP130 and LAMP2 before confocal microscopy visualization. DAPI staining (blue) was performed, showing nuclei.

Supplementary figure 3: Effect of thapsigargin (TG) and cyclopiazonic acid (CPA)) on Golgi morphology, LAMP2 subcellular localisation and glycosylation profile and manganese uptake. A. Immunofluorescence analysis. Control and TMEM165 KO HEK293 cells were incubated with either TG (50nM) or CPA (100µM) for 16h, fixed, permeabilized and labeled with antibodies against GM130, GPP130 and LAMP2 before confocal microscopy visualization. DAPI staining (blue) was performed, showing nuclei. **B.** Control HEK293 cells were incubated with either TG (50nM) or CPA (100µM) for 8h or 16h, in combination or not with 1µM $MnCl_2$. Total cell lysates were prepared, subjected to SDS-PAGE and western blot with the indicated antibodies. **C.** TMEM165 KO HEK293 cells were cultured with either TG (50nM) or CPA (100µM) in combination with 1µM $MnCl_2$ for 16h. Total cell lysates were prepared as described in Material and Methods section for ICP-MS analysis and total manganese concentration was measured (N = 2, n, number of samples = 4).

Figure 5: The N-glycosylation defects observed in TMEM165 KO HEK293 cells treated with TG or CPA are not rescued by Mn^{2+} supplementation. MALDI-TOF-MS spectra of the permethylated N-glycans from TMEM165 KO HEK293 cells following different treatments. **A.** No treatment, **B.** TMEM165 KO HEK293 cells treated with 1µM $MnCl_2$ for 16h, **C. and D.** TMEM165 KO HEK293 cells treated with 50nM TG in combination or not with 1µM $MnCl_2$ for 16h, **E. and F.** TMEM165 KO HEK293 cells treated with 100µM CPA in combination or not with 1µM $MnCl_2$ for 16h. Symbols represent sugar residues as follow: blue square, *N*-acetylglucosamine; green circle, mannose; yellow circle, galactose; purple diamond, sialic acid; red triangle, fucose. Linkages between sugar residues have been removed for simplicity.

Supplementary figure 4: Quantification of the abnormal structures found in TMEM165 KO HEK293 cells treated with TG or CPA with or without Mn^{2+}. A. Quantification of abnormal glycan structures observed in TMEM165 KO HEK293 cells following the different indicated treatments. **B.** Representative glycan structures took into account for the quantification (abnormal structures with mass-per-charge ratios (m/z) 1661, 1835, 2080 and 2326; high mannose structures with mass-per-charge ratios (m/z) 1579, 1783, 1988, 2192 and 2396; complex glycan structures mass-per-charge ratios (m/z) 2227, 2431, 2530, 2605, 2646 and 2891). Symbols represent sugar residues as follow: blue square, *N*-acetylglucosamine; green circle, mannose; yellow circle, galactose; purple diamond, sialic acid; red triangle, fucose. Linkages between sugar residues have been removed for simplicity.

Figure 6: Potential involvement of SERCA2b pump in the Mn^{2+} supplementation effect. Effect of SERCA2b overexpression in control and TMEM165 KO HEK293 cells treated or not with 500µM $CaCl_2$ and 1mM sodium pyruvate on LAMP2 glycosylation. Total cell lysates were prepared, subjected to SDS-PAGE and western blot with the indicated antibodies.

Fig.1

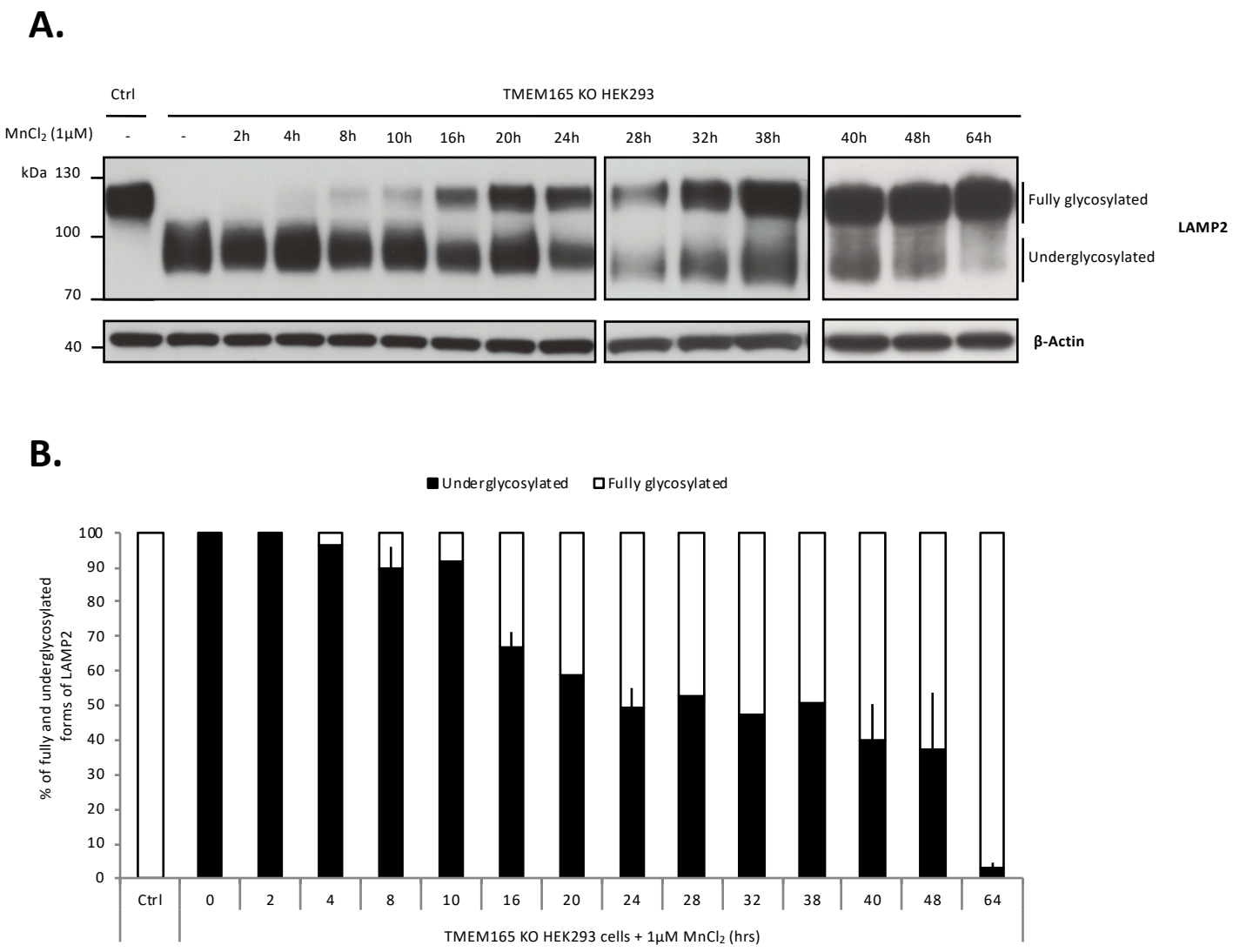

Figure 1: Time course of the Mn^{2+} induced LAMP2 glycosylation rescue. A. Control and TMEM165 KO HEK293 cells were cultured with 1µM $MnCl_2$ during the indicated times. Cell culture medium was renewed every 16h. Total cell lysates were prepared, subjected to SDS-PAGE and western blot with the indicated antibodies. **B.** Relative quantification of fully and underglycosylated forms of LAMP2 (N, number of experiments = 2).

Supplementary fig. 1

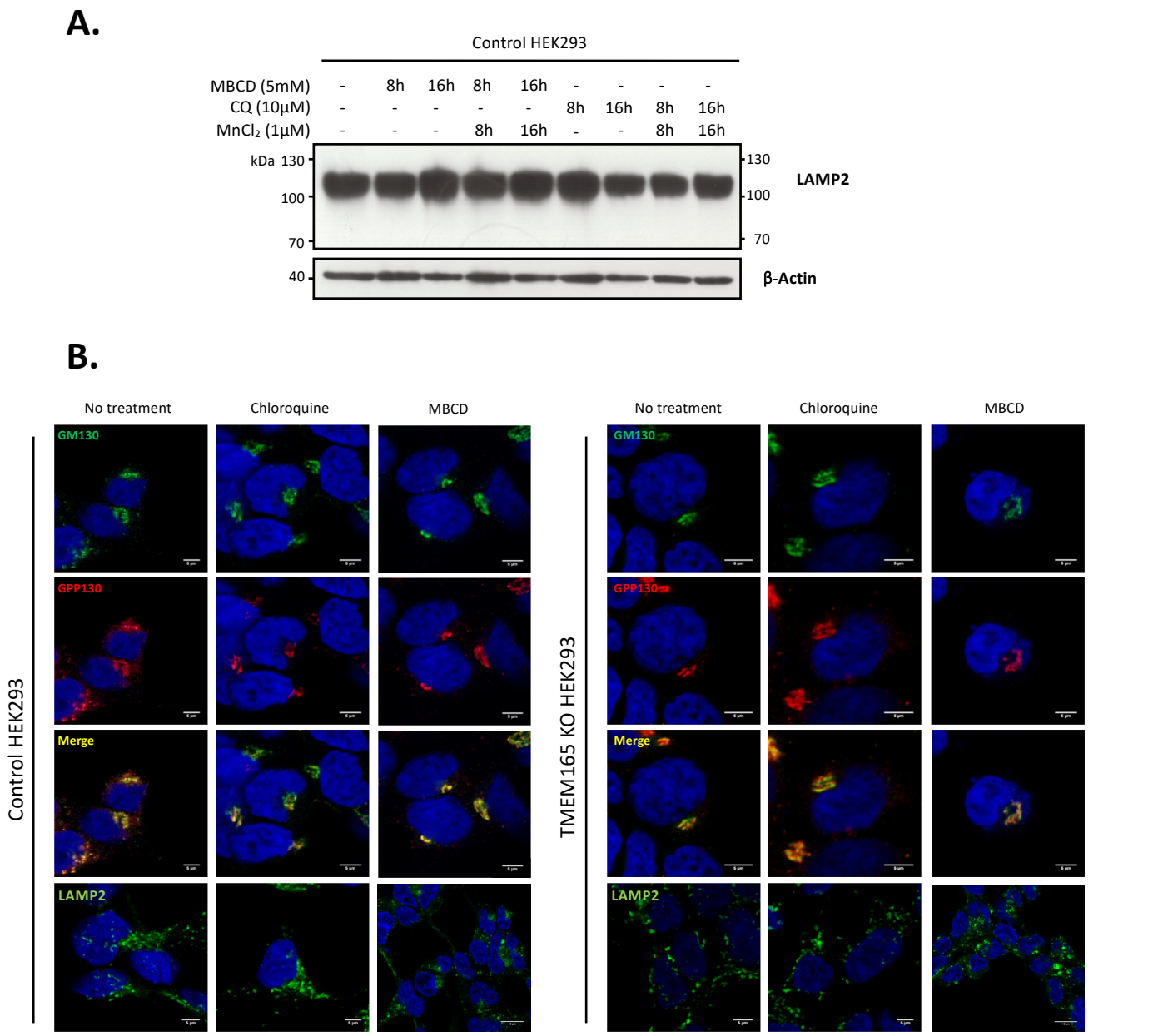

Supplementary figure 1: Effect of chloroquine (CQ) and methyl-β-cyclodextrin (MBCD) on Golgi morphology, LAMP2 subcellular localization and glycosylation profile. A. Control HEK293 cells were incubated with CQ (10µM) or MBCD (5mM) for 8h or 16h, in combination or not with 1µM $MnCl_2$. Total cell lysates were prepared, subjected to SDS-PAGE and western blot with the indicated antibodies. **B**. Immunofluorescence analysis. Control and TMEM165 KO HEK293 cells were incubated with CQ (10µM) or MBCD (5mM) for 16h, fixed, permeabilized and labeled with antibodies against GM130, GPP130 and LAMP2 before confocal microscopy visualization. DAPI staining (blue) was performed, showing nuclei.

Supplementary Fig. 2

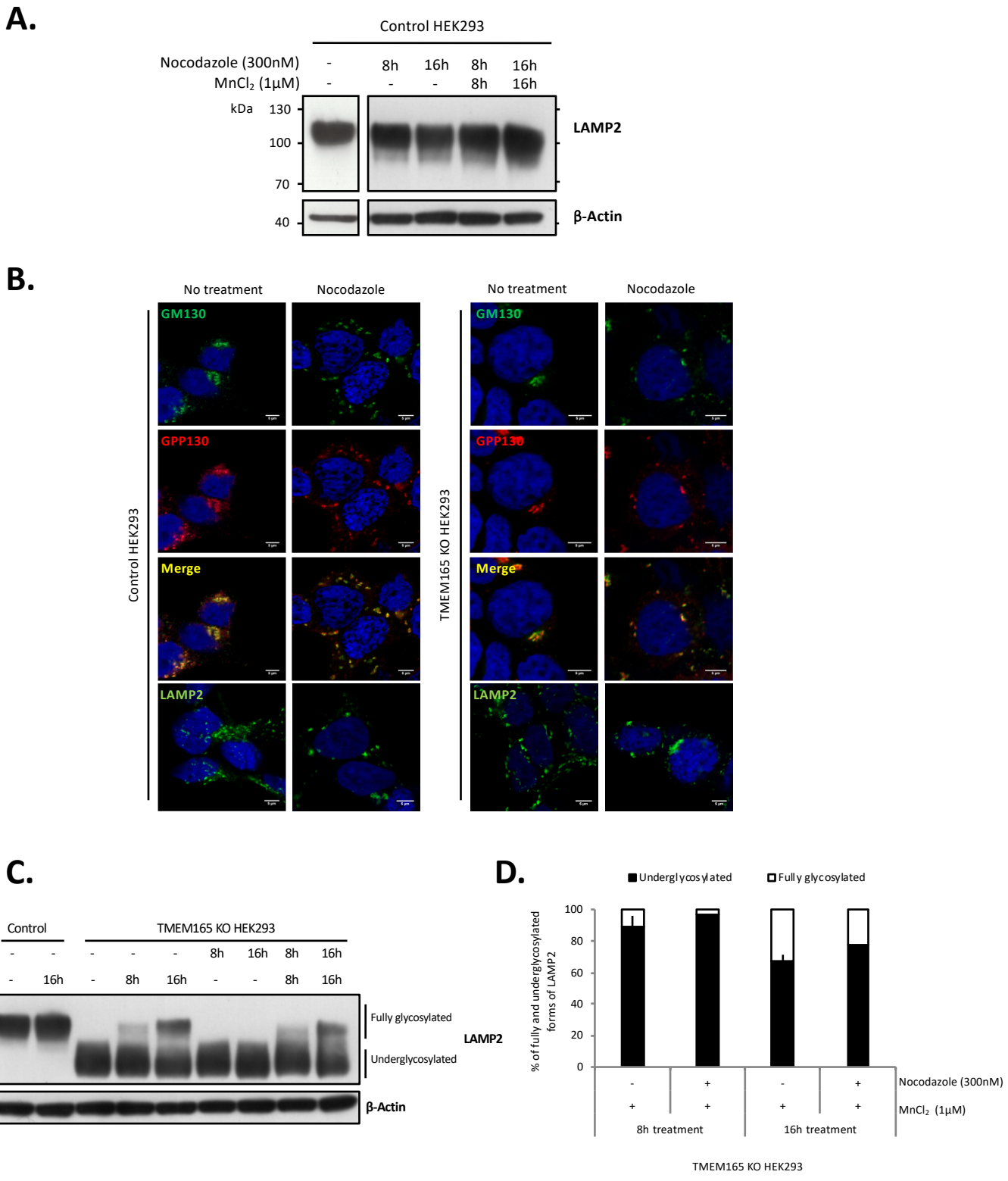

Supplementary figure 2: Effect of nocodazole on Golgi morphology, LAMP2 subcellular localization and glycosylation profile. A. and **C.** Control and TMEM165 KO HEK293 cells were incubated with nocodazole (300nM) for 8h or 16h, in combination or not with 1µM $MnCl_2$. Total cell lysates were prepared, subjected to SDS-PAGE and western blot with the indicated antibodies. **B**. Immunofluorescence analysis. Control and TMEM165 KO HEK293 cells were incubated with nocodazole (300nM) for 16h, fixed, permeabilized and labeled with antibodies against GM130, GPP130 and LAMP2 before confocal microscopy visualization. DAPI staining (blue) was performed, showing nuclei. **D.** Relative quantification of fully and underglycosylated forms of LAMP2 (N, number of experiments = 2).

Fig. 2

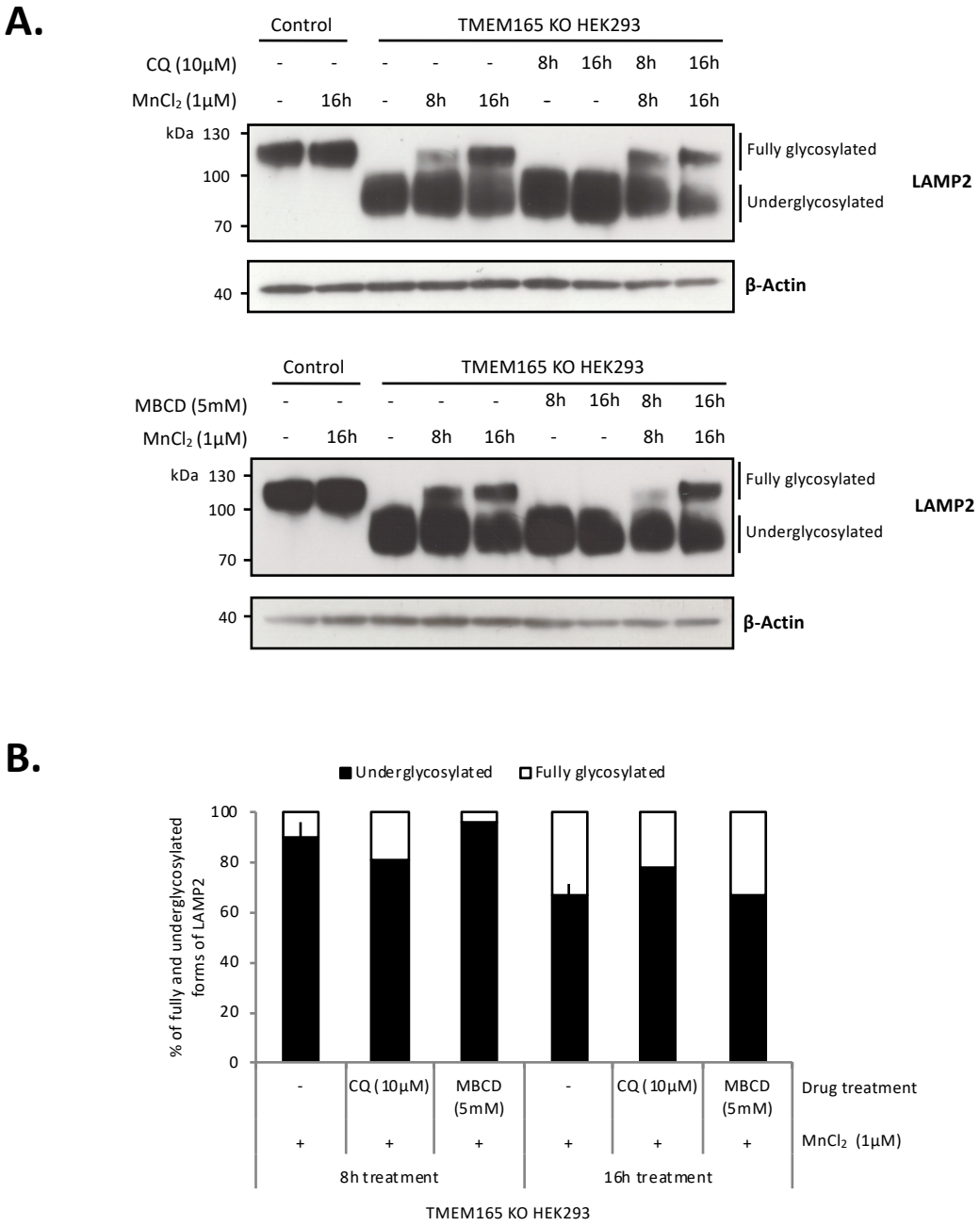

Figure 2: Mn^{2+} entry into TMEM165 KO HEK293 cells does not rely on endocytosis. A. Control and TMEM165 KO HEK293 cells were cultured with CQ (10µM) or MBCD (5mM) in combination or not with 1µM $MnCl_2$ for 8h or 16h. Total cell lysates were prepared, subjected to SDS-PAGE and western blot with the indicated antibodies. **B.** Relative quantification of fully and underglycosylated forms of LAMP2 (N, number of experiments = 2).

Fig. 3

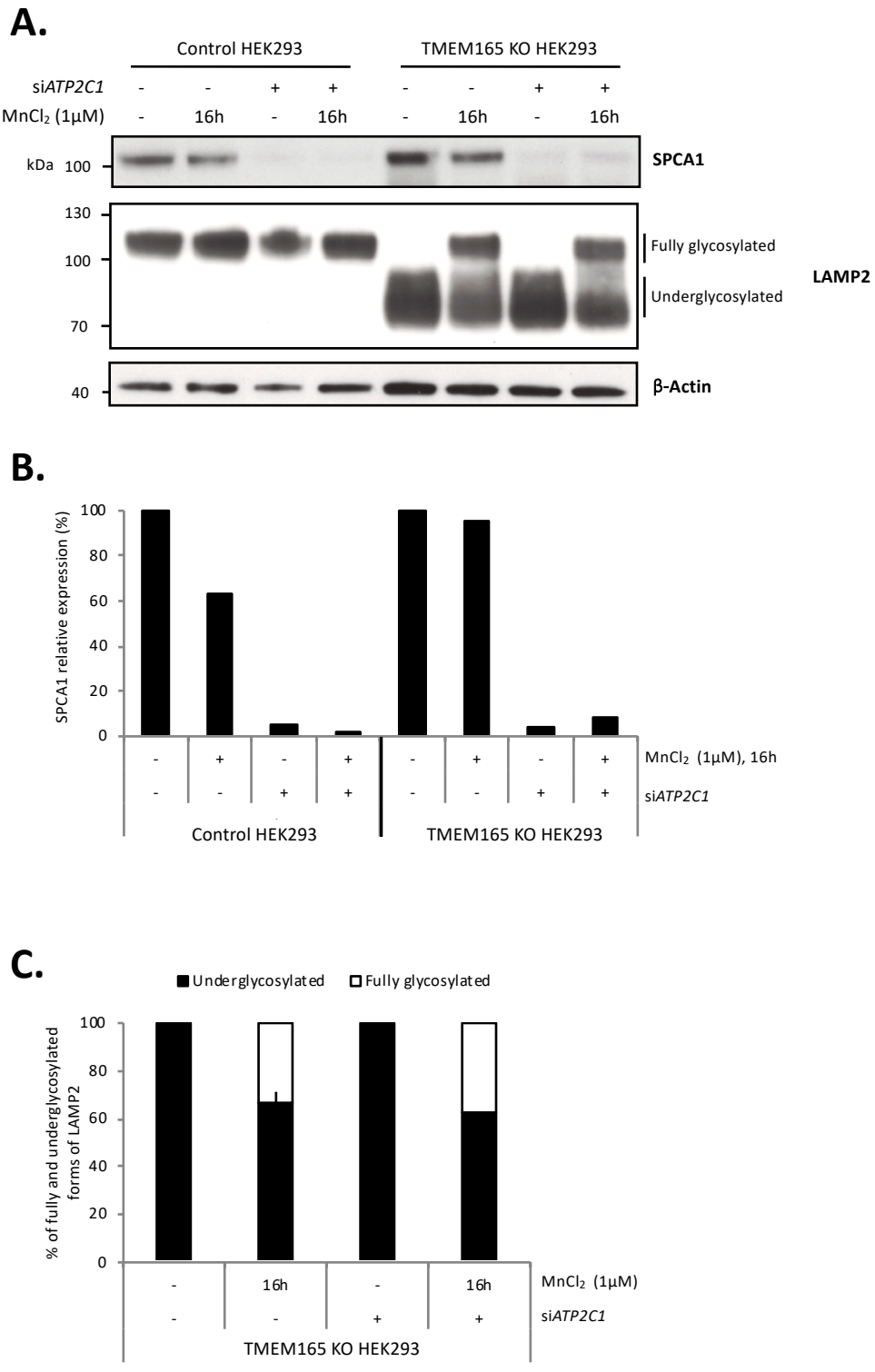

Figure 3: *ATP2C1* knockdown does not prevent the Mn^{2+} induced rescue glycosylation of LAMP2 in TMEM165 KO HEK293 cells. A. Control, TMEM165 KO and si*ATP2C1* HEK293 cells were cultured with 1µM $MnCl_2$ for 16h. Total cell lysates were prepared, subjected to SDS-PAGE and western blot with the indicated antibodies. **B.** Quantification of SPCA1 protein expression after normalization with actin. **C**. Relative quantification of fully and underglycosylated forms of LAMP2.

Supplementary Fig. 3

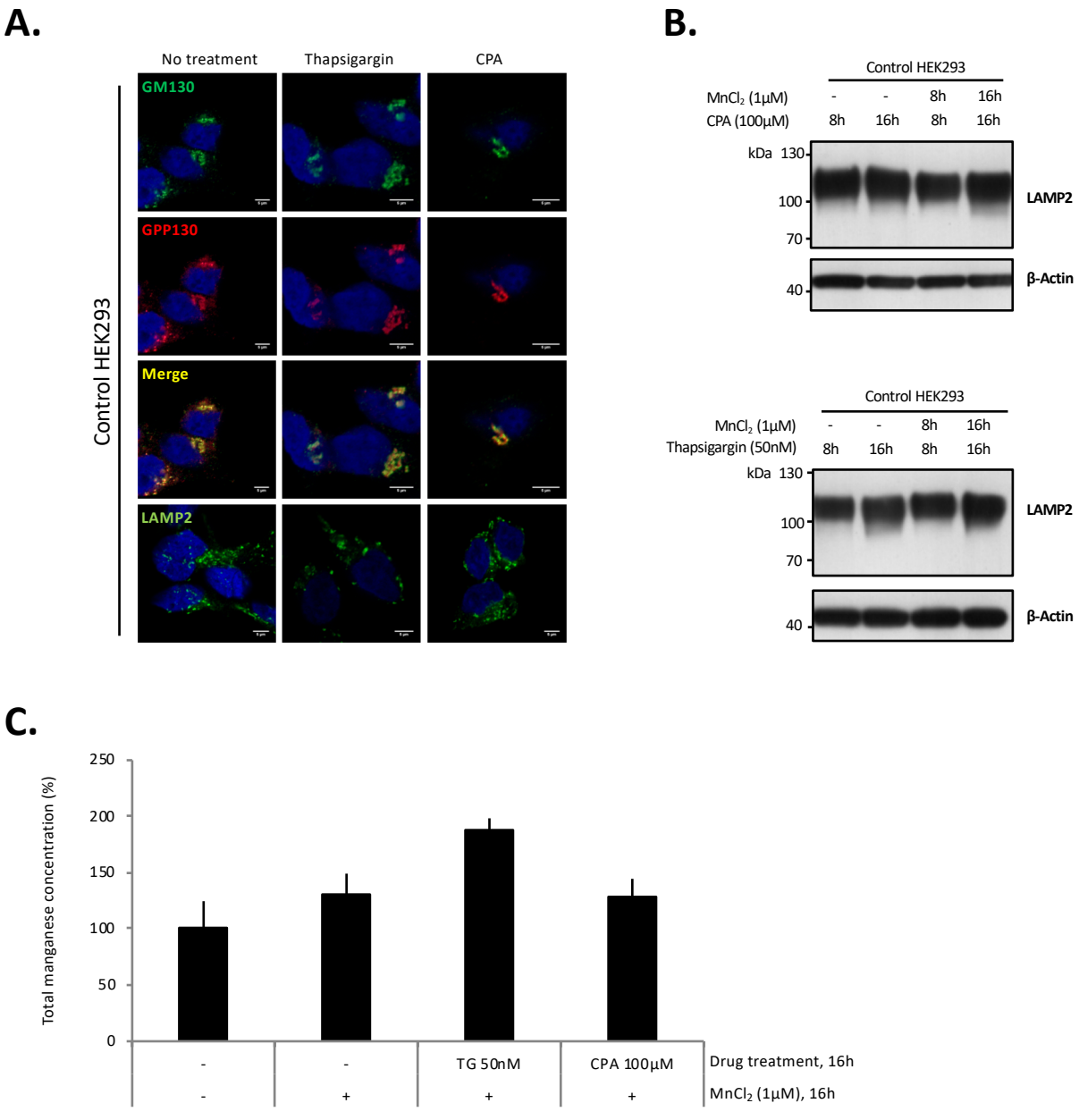

Supplementary figure 3: Effect of thapsigargin (TG) and cyclopiazonic acid (CPA)) on Golgi morphology, LAMP2 subcellular localization and glycosylation profile and manganese uptake. A. Immunofluorescence analysis. Control cells were incubated with either TG (50nM) or CPA (100µM) for 16h, fixed, permeabilized and labeled with antibodies against GM130, GPP130 and LAMP2 before confocal microscopy visualization. DAPI staining (blue) was performed, showing nuclei. **B.** Control HEK293 cells were incubated with either TG (50nM) or CPA (100µM) for 8h or 16h, in combination or not with 1µM $MnCl_2$. Total cell lysates were prepared, subjected to SDS-PAGE and western blot with the indicated antibodies. **C**. TMEM165 KO HEK293 cells were cultured with either TG (50nM) or CPA (100µM) in combination with 1µM $MnCl_2$ for 16h. Total cell lysates were prepared as described in Material and Methods section for ICP-MS analysis and total manganese concentration was measured (N = 2, n, number of samples = 4).

Fig. 4

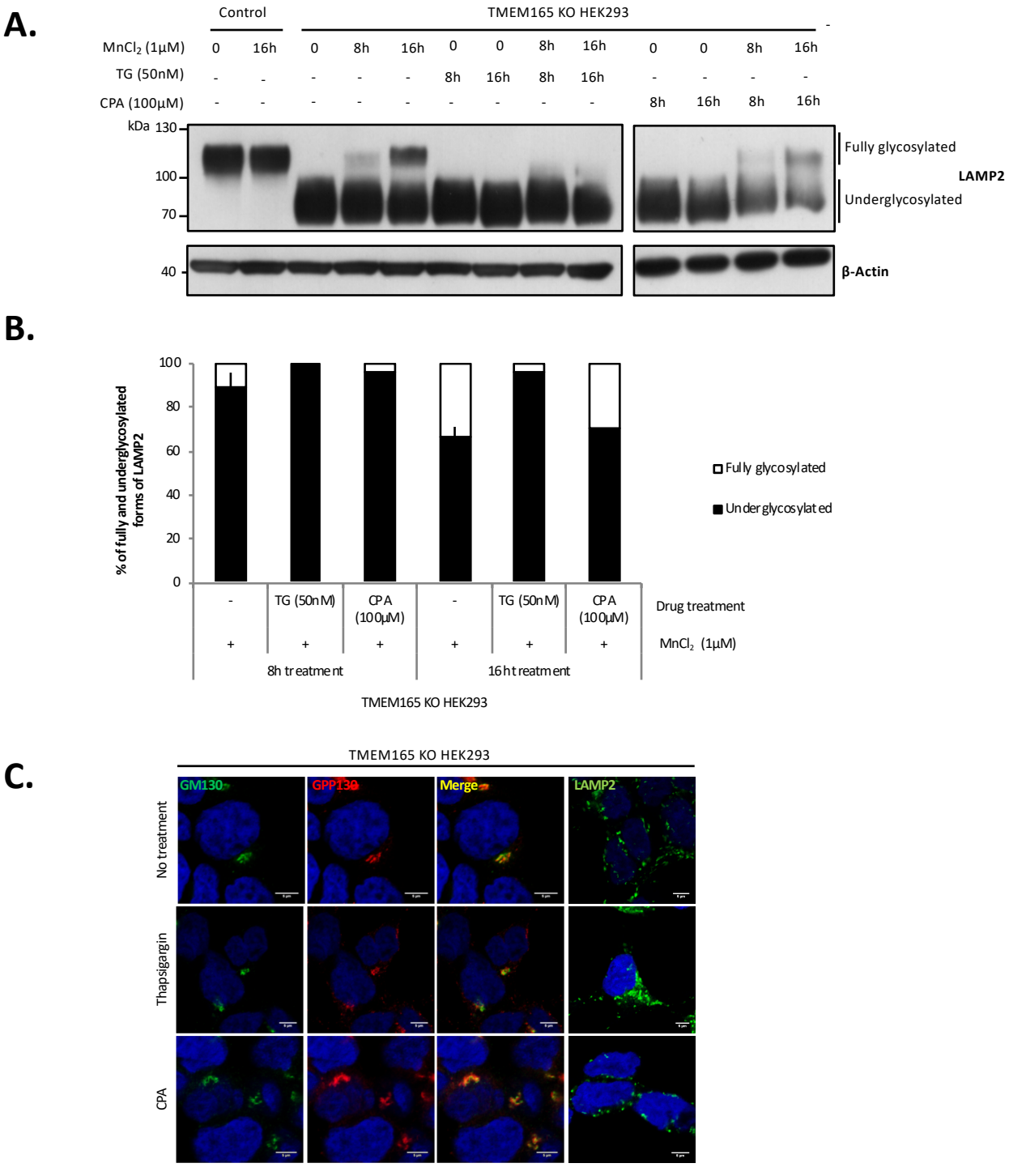

Figure 4: Involvement of TG and CPA sensitive pumps in the Mn^{2+} induced rescue of LAMP2 glycosylation. A. Control and TMEM165 KO HEK293 cells were cultured with either thapsigargine (TG) (50nM) or cyclopiazonic acid (CPA) (100µM), two SERCA inhibitors, in combination or not with 1µM $MnCl_2$ for 8h or 16h. Total cell lysates were prepared, subjected to SDS-PAGE and western blot with the indicated antibodies. **B.** Relative quantification of fully and underglycosylated forms of LAMP2 (N, number of experiment = 2). **C**. Immunofluorescence analysis. TMEM165 KO HEK293 cells were incubated with either TG (50nM) or CPA (100µM) for 16h, fixed, permeabilized and labeled with antibodies against GM130, GPP130 and LAMP2 before confocal microscopy visualization. DAPI staining (blue) was performed, showing nuclei.

Fig. 5

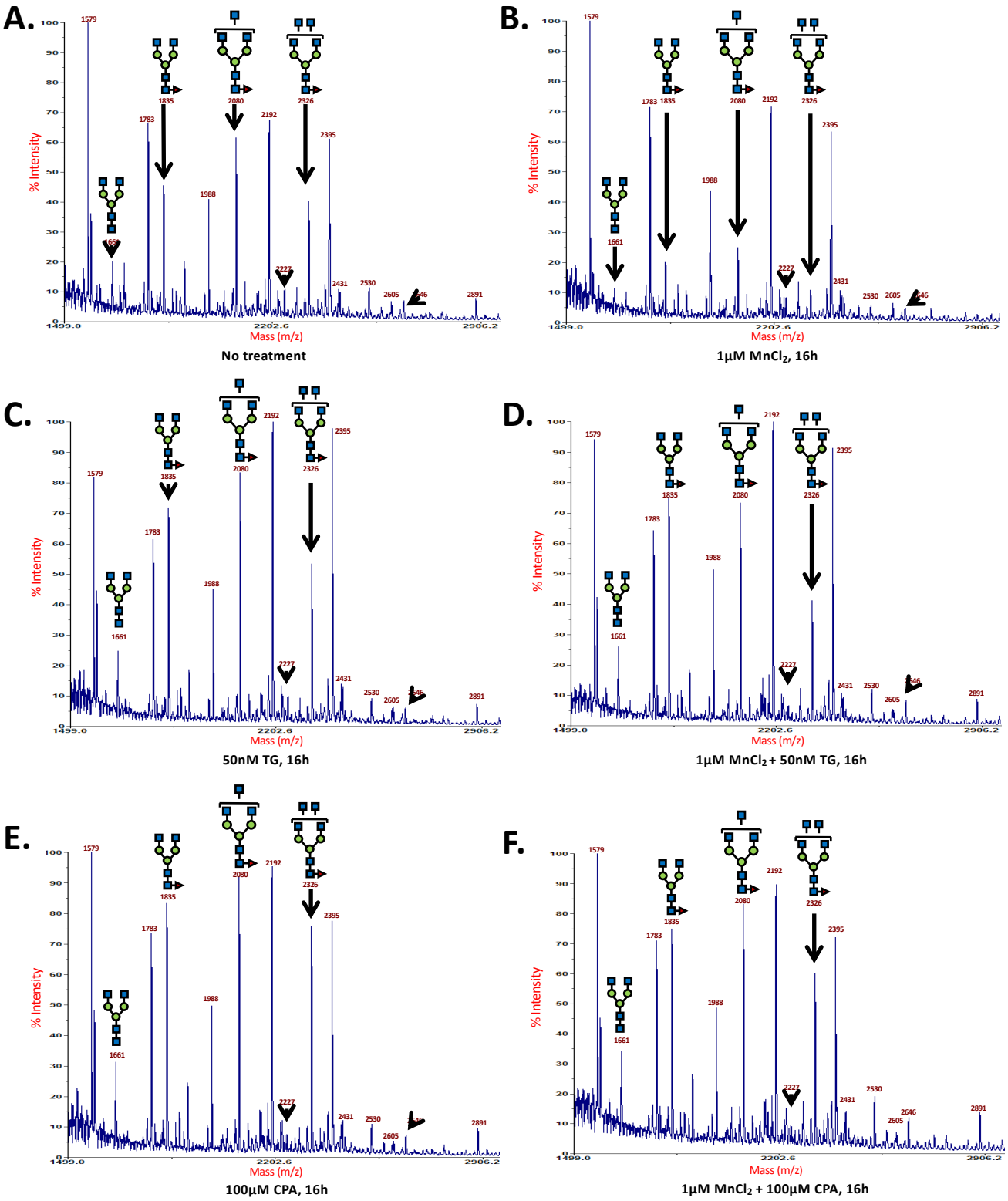

Figure 5: The N-glycosylation defects observed in TMEM165 KO HEK293 cells treated with TG or CPA are not rescued by Mn^{2+} supplementation. MALDI-TOF-MS spectra of the permethylated N-glycans from TMEM165 KO HEK293 cells following different treatments. **A.** No treatment, **B.** TMEM165 KO HEK293 cells treated with 1µM $MnCl_2$ for 16h, **C. and D.** TMEM165 KO HEK293 cells treated with 50nM TG in combination or not with 1µM $MnCl_2$ for 16h, **E. and F.** TMEM165 KO HEK293 cells treated with 100µM CPA in combination or not with 1µM $MnCl_2$ for 16h. Symbols represent sugar residues as follow: blue square, *N*-acetylglucosamine; green circle, mannose; yellow circle, galactose; purple diamond, sialic acid; red triangle, fucose. Linkages between sugar residues have been removed for simplicity.

Supplementary fig. 4

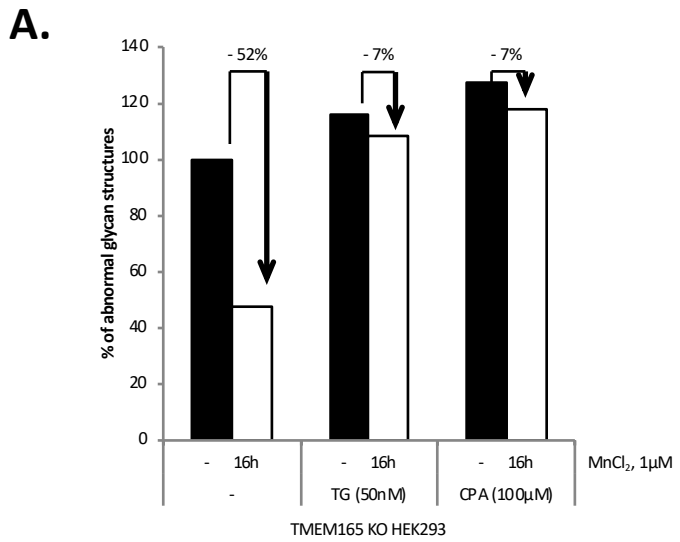

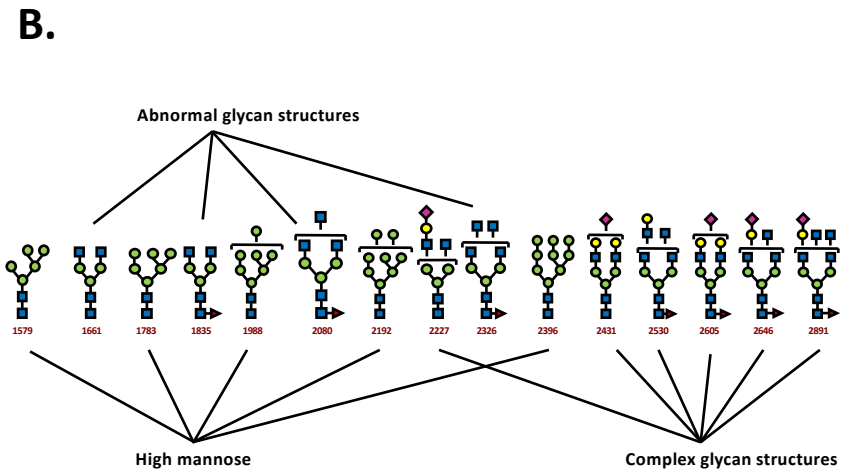

Supplementary figure 4: Quantification of the abnormal structures found in TMEM165 KO HEK293 cells treated with TG or CPA and with or without Mn^{2+}. A. Quantification of abnormal glycan structures observed in TMEM165 KO HEK293 cells following the different indicated treatments. **B.** Representative glycan structures took into account for the quantification (abnormal glycan structures with mass-per-charge ratios (m/z) 1661, 1835, 2080 and 2326; high mannose structures with mass-per-charge ratios (m/z) 1579, 1783, 1988, 2192 and 2396; complex glycan structures mass-per-charge ratios m(/z) 2227, 2431, 2530, 2605, 2646 and 2891). Symbols represent sugar residues as follow: blue square, *N*-acetylglucosamine; green circle, mannose; yellow circle, galactose; purple diamond, sialic acid; red triangle, fucose. Linkages between sugar residues have been removed for simplicity.

Fig. 6

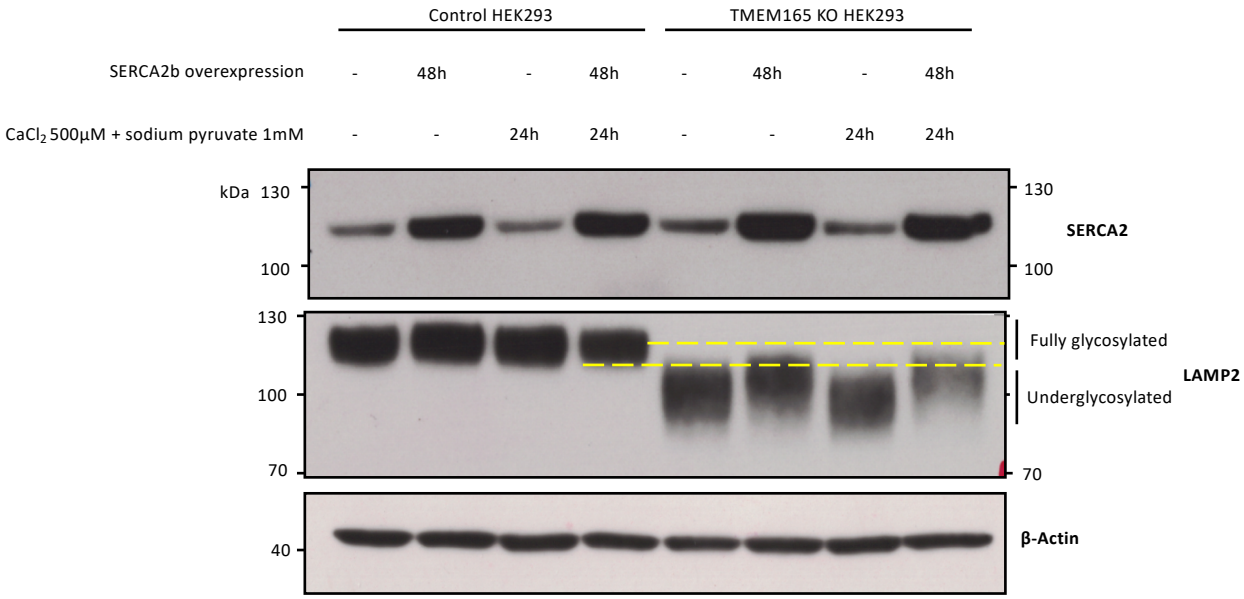

Figure 6: Potential involvement of SERCA2b pump in the Mn^{2+} supplementation effect. Effect of SERCA2b overexpression in control and TMEM165 KO HEK293 cells treated or not with 500µM $CaCl_2$ and 1mM sodium pyruvate on LAMP2 glycosylation. Total cell lysates were prepared, subjected to SDS-PAGE and western blot with the indicated antibodies.